Investigation of influential factors on yield strength of lead rubber bearings

M. Pourmasoud, A. Park
Low Damage Design Co, Hamilton.

I. Hajirasouliha
The University of Sheffield, UK.

J.B.P. Lim
University of Auckland, Auckland.

ABSTRACT

The design of seismic isolators as specified by building code requirements is well defined and well established. However, there is still some refinement required for these design practices, especially in terms of estimating the yield strength and confinement of lead cores. The current codes have specified Upper Bound (UB) and Lower Bound (LB) criteria to encompass variability in the characteristic properties that determine the performance requirements of the isolators. The Lead Core is a key component in a Lead Rubber Bearing (LRB) that provides energy absorption resulting in the damping of a unit/system. Historically, designers have used a standard value for lead yield (8-10 MPa) depending on individual preferences. However, based on prototype test results, it has been shown that lead yielding is variable and strongly influenced by a number of physical parameters. This research has focused on these parameters and determines a new approach to more accurately calculate the Energy Dissipated per Cycle (EDC). Test results of 30 full-scale case studies, including more than 350 compression-shear and tension-shear tests, were critically investigated. The results were then categorised based on confinement conditions, including high, medium, and low confinement, as defined further within this

paper. The results illustrate that appropriate confinement provides a high yield strength level and ultimately an optimised seismic isolation design. The trend of yield strength index versus the stability index was developed and a new equation was proposed to calculate the lead core's yield strength for practical design purposes.

1 INTRODUCTION

In a conventional lead rubber bearing, the lead core is the key component that provides damping. Lead plugs can provide high damping capacity due to their relatively low yield strength of about 10MPa and a perfect elastic-plastic behavior (Skinner et al. 1993). Although 10 MPa is known as a nominal number for lead yield strength (σy), parameters such as the magnitude of applied axial load, dimension of lead core, lateral shear strain of bearing, and the adopted cyclic loads (degradation) also considerably affect the lead yield strength (McVitty et al. 2015). Kelly (2001) proposed 7 to 8.5 MPa as the pragmatic yield level of the lead core depending on the axial load and level of confinement, with 10.5 MPa as the theoretical yield level. Furthermore, it was reported that more shim plates and thinner rubber layers, restrain the lead core from bulging into the rubber layers, which help enhance yield strength along with utilizing confining plates at the top and bottom of the lead core. The multilinear behavior of a lead rubber bearing tends to be bilinear, providing appropriate confinement for the lead core, so a yield strength closer to the nominal value will be achieved.

Kalpakidis et al. (2010), Constantinou et al. (2011) and Arguc et al. (2017) investigated the effect of heating caused by cyclic loading on the characteristic strength of lead cores. It was estimated 10 to 12 MPa yield levels arise from the third cycle of loading depending on lead core size, isolator diameter, and manufacturing details. The value for the first cycle is factored up by 1.35 ($\sigma_{L1} = 1.35\sigma_{L2}$) leading to 13.5 to 16.2 MPa, which are not necessarily consistent with the evidence emerging from real-life projects with the exception of those under low lateral displacements.

2 EXPERIMENTAL CASE STUDIES

More than 350 tests were performed on 30 full-scale isolators to study the effect of influential factors on the lead yield strength. The selected isolators represent a reasonable range of specifications and configurations used in common practice. The isolators were tested under tension, zero, and compressive axial load along with a variety of lateral displacements (less than 50% to more than 200% shear strain). Figure 1 demonstrates a test protocol sample provided for one of the case studies (VLA project). More than twenty tests involving a variety of compression/tension axial loads along with shear strains from 0% up to 200% were considered in this case. In this figure, PT-16 to PT-20 (detailed in Table 1) are used to

investigate the effect of axial load on stiffness and damping under constant lateral displacement. As was expected, by increasing the axial load, the lateral stiffness decreases. It is worth mentioning that, although Ryan et al. (2005) reported zero damping in the case of tension mechanism (presented in the introduction), the isolators under zero/tension plus shear loads still provided an appropriate degree of damping, which usually is disregarded during the design process.

Item	Descrip.	Sequence	Axial Load	Deformation			Frequency	# Cycles
			(kN)	Desc.	Δ (mm)	γ (%)	(Hz)	
Prototype Test Sequence and Cycles (Cl. 17.8.2.2)								
Compression stiffness								
1	Comp	PT-00	11500	-	-	0%	-	2
Wind Stability, Performed Quasi-Statically								
2	Wind	PT-01	4800	Wind	10	3%	-	20
Cyclic Load Tests to Establish Force-Deflection Behavior, Performed Quasi-Statically or Dynamically								
3	Seismic Static	PT-02	4800	$0.25D_M$	150	43%	-	3
		PT-03	4800	$0.5D_M$	300	86%	-	3
		PT-04	4800	$0.67D_M$	402	115%	-	3
		PT-05	4800	$1.0D_M$	600/150	171%	-	3
4	Seismic	PT-06	8450	$1.0D_M$	600/150	171%	-	3
		PT-07	20600	$1.0D_M$	600/150	171%	-	3
		PT-08	-1250	$1.0D_M$	600/150	171%	-	3
Cyclic Load Tests to Check Durability, Performed Quasi-Statically or Dynamically								
5	Repeat	PT-09	4800	$0.75D_M$	450	129%	-	10
Load Test of Isolator Stability, Performed Quasi-Statically								
6	Max	PT-10	20600	$1.1D_{TM}$	700/150	200%	-	1
	Min	PT-11	-1250	$1.1D_{TM}$	700/150	200%	-	1
	Comp	PT-12	20600	-	-	0%	-	2
Repeat tests								
7	Comp	PT-13	11500	-	-	0%	-	2
	Seismic	PT-14	4800	$0.67D_M$	402	115%	-	3
	Seismic	PT-15	-750	$0.67D_M$	402	115%	-	3
Compression - Shear tests								
8	Compression Variation	PT-16	0	$0.67D_M$	402	115%	-	3
		PT-17	4800	$0.67D_M$	402	115%	-	3
		PT-18	8450	$0.67D_M$	402	115%	-	3
		PT-19	15000	$0.67D_M$	402	115%	-	3
		PT-20	20600	$0.67D_M$	402	115%	-	3
Tension - Shear tests								
9	Tension Variation	PT-21	0	$0.67D_M$	402	115%	-	3
		PT-22	-750	$0.67D_M$	402	115%	-	3
		PT-23	-1250	$0.67D_M$	402	115%	-	3

Figure 1: Test protocol sample

Table 1 demonstrates the variation of effective stiffness and effective damping over 21 cycles of loading in Tests 16 to 20. In general, the results indicate that increasing the axial load leads to better confinement and subsequently more damping. In the meantime, zero/tension axial loads (Tests 16, 21, and 22) degraded the damping ratio up to 50%, although its effect on the effective stiffness was negligible.

Table 1: Influence of axial load variation on effective stiffness and damping (prototype tests for VLA case in Table 1).

	Axial load (kN)	Disp Min (mm)	Disp Max (mm)	Load Min (kN)	Load Max (kN)	Area (kNm)	k effective (kN/mm)	Damping %
PT-16	0	-402.2	403.2	-934	896	402.3	2.3	17.4
PT-17	4800	-402.2	403.2	-973	884	531.1	2.3	22.6
PT-18	8450	-402.2	403.2	-956	854	551.9	2.2	24.1
PT-19	15000	-402.2	403.2	-902	783	578.7	2.1	27.2
PT-20	20600	-402.2	403.1	-833	712	594.4	1.9	30.4
PT-21	0	-402.2	402.9	-884	844	367.5	2.1	16.8
PT-22	-750	-402.2	402.7	-869	837	292.6	2.1	13.6

For instance, Figure 2 compares the hysteresis loops of the VLA isolators under the maximum, zero, and minimum axial loads. It is observed that increasing the axial load causes the hysteresis loop shape to turn from multilinear to a quasi bilinear behaviour. Observation of necking in the hysteresis loops indicates the lack of axial load on the bearing. In other words, when the applied axial load is not in proportion with the isolator size, a hysteresis loop with necking behaviour will be expected because of a lack of confinement on the lead core. This can influence the energy dissipation capacity of the isolator and needs to be considered in the design process.

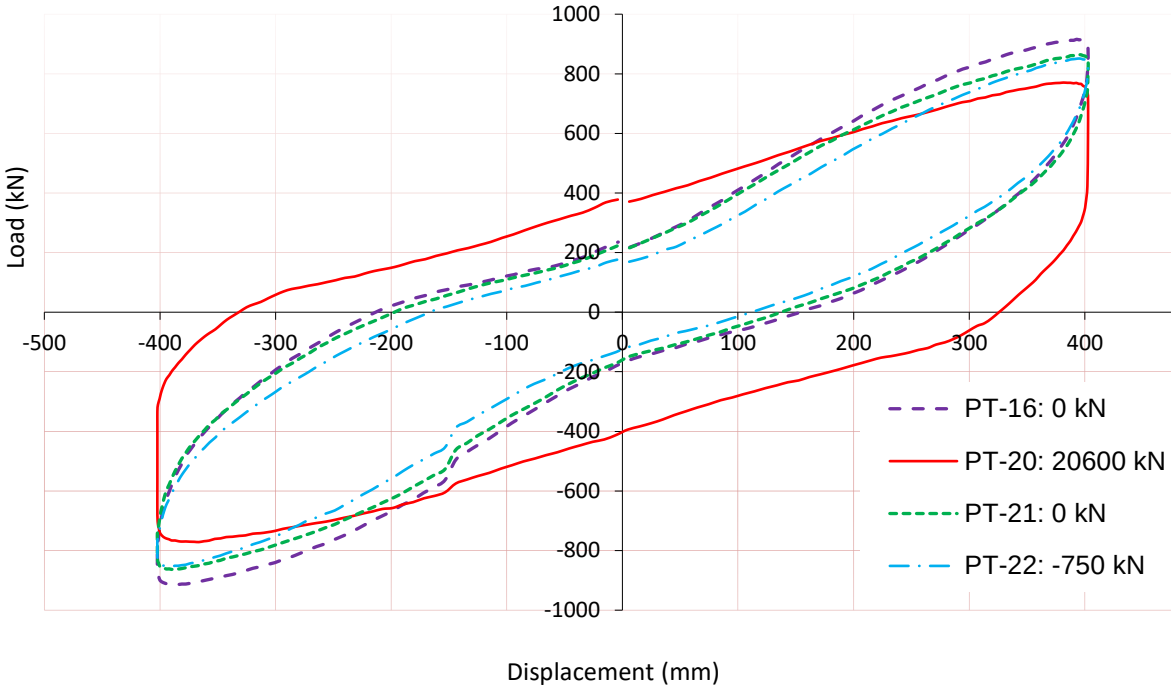

Figure 2: Hysteresis loops of the maximum, minimum and zero axial load tests.

The actual yield strength (σy) and characteristic strength (Q_d) of a lead rubber bearing are achievable through hysteresis loops extracted from experimental tests. These parameters are a function of the applied conditions including (but not restricted to) the magnitude of axial load, slenderness of the lead core, applied shear strength, the thickness of rubber layers, the shear modulus of the rubber, and the top and bottom confinement of the lead core. The influential factors are incorporated in the buckling load P_{cr} as per Equation 1.

$$P_{cr} = \frac{\lambda\, G\, A_r\, a\, S}{T_r} \qquad (1)$$

where λ is 1.1 for bearings with holes, G is the rubber shear modulus, A_r is the reduction area that depends on the lateral displacement, a is the effective width of the bearing, and S is the shape factor that depends on the thickness and dimension of the rubber layers. Any change in the aforementioned parameters affects lead core confinement and lead core yield strength. Therefore, P_{cr} can be deemed as an indication to estimate the effect of influential factors on the yield strength.

Figure 3 shows the results extracted from all the selected tests. The vertical axis represents the normalised characteristic strength (Q/Q_0) which starts from one for the compression loads and

has a direct relationship with the compression axial load. The horizontal axis is the normalized axial load ($^{P}/_{P_0}$) which is the ratio of applied load over the isolator's buckling capacity. The diagrams offer different slopes which represent a variety of confinement conditions of the lead cores.Generally, three different trends are recognised. The green line represents Low Confinement (LC) and low yield strength. The characteristic strength, even under high axial loads ($^{P}/_{P_{cr}} > 0.5$), is approximately 20% more than the characteristic strength under zero axial load ($^{Q}/_{Q_0} = 1.2$). It should be noted that for all the case studies, the axial loads under seismic load combinations were more than 50% of the buckling load. The orange dots show the High Confinement (HC) trend with normalised characteristic strength of more than 1.6. The yield strength of this category is quite close to the theoretical yield strength (10 MPa). The outcomes between the two aforementioned categories (green and orange) are designated Medium Confinement (MC) and their normalised characteristic strength values lie between 1.2 and 1.6.

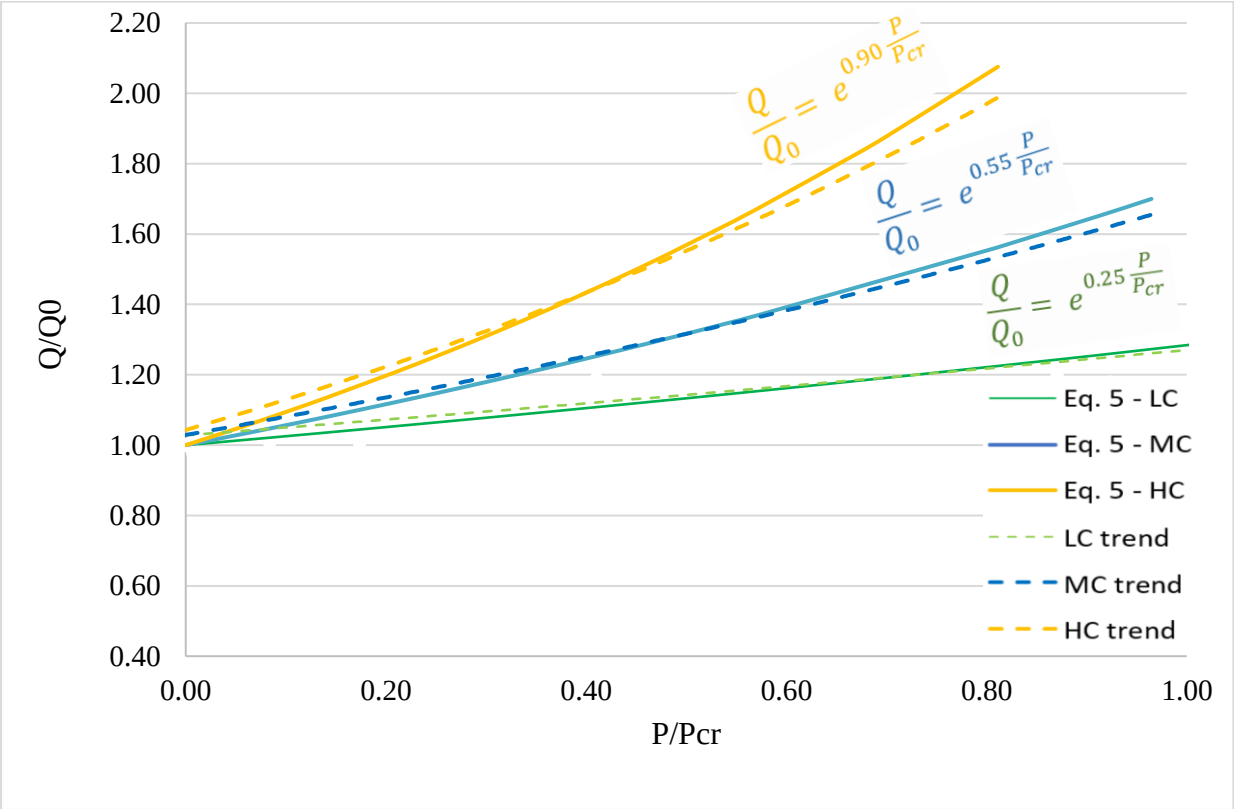

Figure 3: Confinement categories and their effect on the normalized characteristic strength

Based on the results presented in Figure 3, for each confinement category the characteristic strength of a lead rubber bearing is achievable through Equation 2.

$$\frac{Q}{Q_0} = e^{\alpha \frac{P}{Pcr}} \quad (2)$$

where α is the confinement exponent that is 0.25 for low confinement, 0.55 for medium confinement, and 0.90 for high confinement. Figure 3 compares the trends regarding Equation 2 (dashed lines) with the data obtained for each confinement category. The tests' results demonstrate that the yield strength under zero axial loading is almost constant and can be assumed around 6.0 MPa (±10% as UB and LB) regardless of the confinement category.

Two main factors including slenderness ratio ($^{Hcore}/_{D_{core}}$) and the area ratio ($^{A_l}/_{A_b}$), were defined to address the conditions that affects the yield strength under the zero axial load. where H is the lead core height, D_{core} is the lead core diameter, A_l is the cross area of the lead core, and A_b is the bonded area of the isolator. In addition, the slenderness ratio over the area ratio is defined as Influential Factor Ratio (IFR). Generally, IFR is less and 1.0 for low confinement, and is expected to be more than 2.0 and 7.0 for medium and high confinements, respectively.

Fig. **4** illustrates the trend for σ_{y0} versus IFR when an accurate yield strength is known. The diagram has a steep slope for IFRs less than one but changes to a smoother slope with increasing IFR, which indicates that the axial load influence is more significant for fewer IFRs. In other words, better confinement results in less variation of yield strength regardless of the axial load. To obtain the yield strength under zero axial load, $\sigma_{y0} = 0.35\ln(IFR)$+6 (3 3 can be employed:

$$\sigma_{y0} = 0.35\ln(IFR) + 6 \quad (3)$$

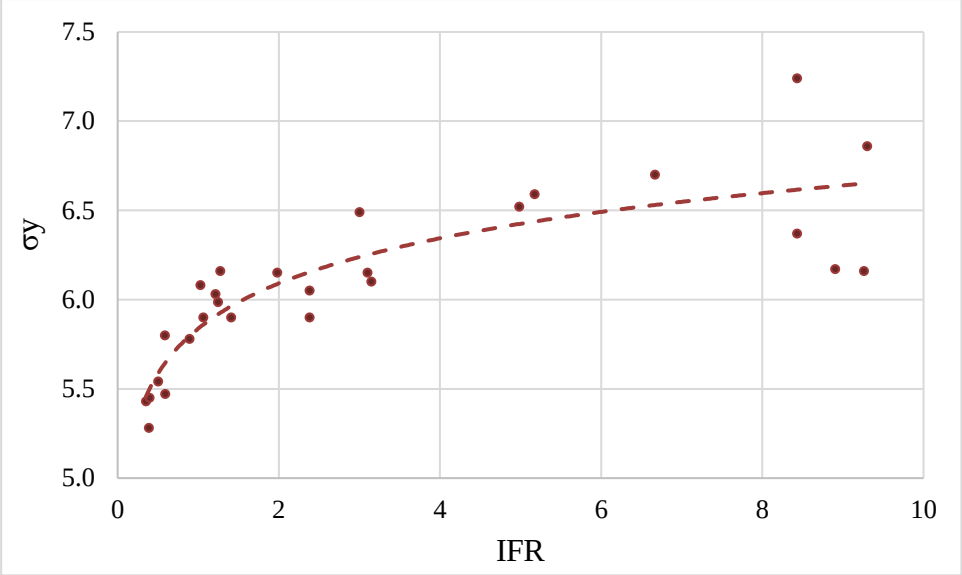

Fig. 4 The trend of yield strength versus IFR based on Equation 3.

Combination of Equation 2 and 3 results in the following equation to calculate the yield strength of lead rubber bearings as a function of their configuration, the imposed axial loads, and other influential factors.

$$\sigma_y = [0.35\ln(IFR) + 6]e^{\alpha\frac{P}{P_{cr}}} \quad (4)$$

Equation 4 provides a practical perspective regarding the actual yield strength of the lead core before running the prototype tests. This equation can help to narrow the gap between upper/lower bounds of λ_{test} and λ_{spec} mentioned in (ASCE 7-16), which is beneficial for the design of super-structures as discussed before.

Conclusion

Lead core plays an important role in the performance of Lead Rubber Bearings (LRB) as it provides the damping effect of the system. Underestimation of the lead core's yield strength causes insufficient damping and extra travel on the isolation level, while overestimation produces a stiff system that transmits unfavorable base shear to the super-structure. The yield strength of the lead core is suggested to be between 6 to 10 MPa in current codes/guidelines depending on loading conditions. Yield strength can be calculated from the hysteresis loops that are obtained from prototype tests. However, there can be incompatibilities between the design targets and test results. This study investigated more than 300 tests to develop a new

approach to estimate the yield strength of lead cores with high accuracy prior to prototype testing.

The following conclusions were made based on the new approach:

- Lead rubber bearings are energy dissipative even under zero/tension and shear actions. While the hysteresis loops of isolators under tension/zero axial loadings are not as inflated as an isolator under heavy axial loading (particularly those with $P/P_{cr} > 0.5$), they still provide a reasonable amount of damping. Currently this effect is neglected in the design process of lead rubber bearings.
- A variety of influential factors, including applied axial load, slenderness of the lead core, and thickness of the rubber layers, confer different levels of confinement for the lead core. Three confinement categories were recognised based on the trend of the normalised characteristic strengths versus the normalised axial loads. The developed Influential Factor Ratio (IFR) shows that IFRs less than 1.0 represent low confinement, IFRs of approximately 2.0 indicate medium confinement, and when IFR exceeds 7.0, high confinement is achieved.
- The yield strength of the lead core directly depends on the level of confinement, the isolator travel amplitude, and the applied axial load. These effects are generally ignored in the code specified design criteria. To address this issue, a new design equation was developed to estimate lead core yield strength by taking into account all the key influential factors.

REFERENCES

Arguc, S., O. Avsar, and G. Ozdemir. 2017. "Effects of Lead Core Heating on the Superstructure Response of Isolated Buildings." *Journal of Structural Engineering* 143 (10): 04017145. https://doi.org/10.1061/(ASCE)ST.1943-541X.0001880.

ASCE. 2016. Minimum Design Loads and Associated Criteria for Buildings and Other Structures. ASCE/SEI 7-16. Reston, VA: ASCE.

Belash, T. A., V. V. Kostarev, J. L. Rutman, and A. M. Uzdin. 2019. "Development of Seismic Isolation in Russia." *16th World Conference on Seismic Isolation, Energy Dissipation and Active Vibration Control of Structures.* St Petersburg. Russian Federation.

Bhagat, S., A. C. Wijeyewickrema, and N. Subedi. 2018. "Influence of Near-Fault Ground Motions with Fling-Step and Forward-Directivity Characteristics on Seismic Response of Base-Isolated Buildings." *Journal of Earthquake Engineering* 0 (0): 1–20. https://doi.org/10.1080/13632469.2018.1520759.

BS EN 1337-3. 2005. Structural Bearings - Part 3*: Elastomeric Bearings*. BSI Standard Publication.

BS EN 1337-5. 2005. *Structural Bearings - Part 5: Pot Bearings*. BSI Standard Publication.

BS EN 15129. 2018. European Standard on Anti-Seismic Devices. BSI Standard Publication.

Constantinou, M.C. I. Kalpakidis, A. Filiatrault, and R.A. Ecker Lay. 2011. LRFD-Based Analysis and Design Procedures for Bridge Bearings and Seismic Isolators. MCEER 11-0004. Buffalo, NY: Univ. at Buffalo.

Du, K., W. Bai, J. Bai, and D. Yan. 2021. "Comparative Seismic Performance Assessment of Reinforced Concrete Frame Structures with and without Structural Enhancements Using the FEMA P-58 Methodology." *ASCE-ASME Journal of Risk and Uncertainty in Engineering Systems* 7 (4).

FEMA. 2003. Multi-Hazard Loss Estimation Methodology - Earthquake Model. HAZUS-MH MR4 Technical Manual, Federal Emergency Management Agency, Washington, DC: FEMA.

FEMA. 2007. Design Guide for Improving Hospital Safety in Earthquakes, Floods, and High Winds: Providing Protection to People and Buildings. FEMA 577. Washington, DC: FEMA.

FEMA. 2018. Building the Performance You Need. FEMA P-58-7. Washington, DC: FEMA.

Jampole, E., S. Swensen, E. Miranda, and G. G. Deierlein. 2020. "Parametric Study of Seismic Isolation Properties for Light-Frame Houses." *Journal of Structural Engineering* 146 (10): 04020207. https://doi.org/10.1061/(ASCE)ST.1943-541X.0002651.

JIS K 6410-1. 2011. Elastomeric Seismic-Protection Isolators for Buildings - Part 1: Specifications. Japanese Standards Association. JIS.

JIS K 6410-2. 2011. Elastomeric Seismic-Protection Isolators for Buildings-Part 2: Test Methods. Japanese Standards Association. JIS.

Kalpakidis, I. V., M. C. Constantinou, and A.S. Whittaker. 2010. "Modeling Strength Degradation in Lead–Rubber Bearings under Earthquake Shaking." *Earthquake Engineering & Structural Dynamics* 39 (13): 1533–49. https://doi.org/10.1002/eqe.1039.

Kelly, T. E. 2001. Base Isolation Design of Structures: Design Guidelines. Holmes Consulting Group ltd.

Kumar, M., A. S. Whittaker, and M. C. Constantinou. 2015. "Experimental Investigation of Cavitation in Elastomeric Seismic Isolation Bearings." *Engineering Structures* 101 (October): 290–305. https://doi.org/10.1016/j.engstruct.2015.07.014.

Mazza, F. 2017. “Behaviour during Seismic Aftershocks of r.c. Base-Isolated Framed Structure with Fire-Induced Damage.” *Engineering Structures* 140 (6): 458–72. https://doi.org/10.1016/j.engstruct.2017.03.008.

Mazza, F., and M. Mazza. 2017. “Seismic Retrofitting by Base-Isolation of r.c. Framed Buildings Exposed to Different Fire Scenarios.” *Earthquakes and Structures* 13 (3): 267–77. https://doi.org/10.12989/eas.2017.13.3.267.

McVitty, W. J., M. C. Constantinou. 2015. Property Modification Factors for Seismic Isolators: Design Guidance for Buildings. MCEER-15-0005. Buffalo, NY: Univ. at Buffalo.

Özuygur, A. R., and E. N. Farsangi. 2021. “Influence of Pulse-Like Near-Fault Ground Motions on the Base-Isolated Buildings with LRB Devices.” *Practice Periodical on Structural Design and Construction* 26 (4): 04021027. https://doi.org/10.1061/(ASCE)SC.1943-5576.0000603.

Pal, S., A. Hassan, and D. Singh. 2019. “Optimization of Base Isolation Parameters Using Genetic Algorithm.” *Journal of Statistics and Management Systems* 22 (7): 1207–22. https://doi.org/10.1080/09720510.2019.1614338.

Pourmasoud, M. M., J. B. P. Lim, I. Hajirasouliha, and D. McCrum. 2020. “Multi-Directional Base Isolation System for Coupled Horizontal and Vertical Seismic Excitations.” *Journal of Earthquake Engineering*. January 1–26. https://doi.org/10.1080/13632469.2020.1713925.

Ryan, K. L., J. M. Kelly, and A. K. Chopra. 2005. “Nonlinear Model for Lead–Rubber Bearings Including Axial-Load Effects.” *Journal of Engineering Mechanics* 131 (12): 1270–78. https://doi.org/10.1061/(ASCE)0733-9399(2005)131:12(1270).

Skinner, R. I., W. H. Robinson, and G. H. McVerry. 1993. An Introduction to Seismic Isolation. Wiley.

Wang, H., W. Zheng, J. Li, and Y. Gao. 2019. “Effects of Temperature and Lead Core Heating on Response of Seismically Isolated Bridges under Near-Fault Excitations.” *Advances in Structural Engineering* 22 (14): 2966–81. https://doi.org/10.1177/1369433219855914.

Weisman, J., and G. P. Warn. 2012. “Stability of Elastomeric and Lead-Rubber Seismic Isolation Bearings.” *Journal of Structural Engineering* 138 (2): 215–23. https://doi.org/10.1061/(ASCE)ST.1943-541X.0000459.

Whittaker, D., W. Parker, D. Pettinga, D. Pierta, G. McVerry, G. Sidwell, A. Cattanach, A. Charleson, W. K. Kam. 2019. Guideline for the Design of Seismic Isolation Systems for Buildings. New Zealand Society for Earthquake Engineering.

Xie, L., X. Wang, D. Zeng, J. Jia, and Q. Liu. 2022. “Resilience-Based Retrofitting of Adjacent Reinforced Concrete Frame–Shear Wall Buildings Integrated into a Common Isolation System.” *Journal of Performance of Constructed Facilities* 36 (1): 04021100. https://doi.org/10.1061/(ASCE)CF.1943-5509.0001678.

Xu, Z., Y. Guo, S. Wang, and X. Huang. 2013. “Optimization Analysis on Parameters of Multi-Dimensional Earthquake Isolation and Mitigation Device Based on Genetic Algorithm.” *Nonlinear Dynamics* 72 (4): 757–65. https://doi.org/10.1007/s11071-013-0751-9.

Yakut, A., and J. A. Yura. 2002. “Parameters Influencing Performance of Elastomeric Bearings at Low Temperatures.” *Journal of Structural Engineering* 128 (8): 986–94. https://doi.org/10.1061/(ASCE)0733-9445(2002)128:8(986).